JOURNAL OF GEOPHYSICAL RESEARCH, VOL. 100, NO. A7, PAGES 11,831–11,843, JULY 1, 1995

Low-altitude observations and modeling of quasi-steady magnetopause reconnection

T. G. Onsager

Institute for the Study of Earth, Oceans, and Space and the Department of Physics, University of New Hampshire, Durham

Shen-Wu Chang and J. D. Perez

Physics Department, Auburn University, Auburn, Alabama

J. B. Austin and L. X. Janoo

Institute for the Study of Earth, Oceans, and Space and the Department of Physics, University of New Hampshire, Durham

Abstract. Data from two near-conjugate passes of DE 1 and DE 2 through the cusp/cleft region of the Earth's magnetosphere are presented and compared with model calculations of particle transport from the solar wind to spacecraft locations in the magnetosphere. Comparison of the observed and calculated particle spectra shows that the model can successfully match the spectra at both spacecraft using the same model parameters. This demonstrates that the modeling technique is applicable at both high and low altitudes. We are also able to conclude that the particles originate from a fairly narrow spatial region on the magnetopause even though magnetosheath plasma has access to the magnetosphere over the entire magnetopause in the model. The success of the model in reproducing key features of the observed spectra and the fact that the two satellites in near magnetic conjunction but at different altitudes observed similar, distinctive features at times separated by 10 - 20 min demonstrates that there are quasi-stationary, spatial features in the cusp/cleft region of the Earth's magnetosphere.

1. Introduction

The injection of plasma particles from the magnetosheath across the magnetopause is an important source of plasma in the Earth's magnetosphere. Measurements of this particle entry process have been made in the dayside low-latitude region [*Sonnerup et al.*, 1981], the dawn and dusk flanks [*Gosling et al.*, 1986], the cusps [*Hill and Reiff*, 1977], and the high-latitude plasma mantle [*Rosenbauer et al.*, 1975; *Newell et al.*, 1991a]. The cusp/cleft region of the Earth's magnetosphere is of special interest because particles from the magnetosheath have more or less direct access and because it is a highly structured region in which field lines map from various other regions of the magnetosphere.

Using particle data from the DMSP satellites, *Newell et al.* [1991a, b] have identified a number of distinct magnetospheric regions in the low-altitude cusp/cleft. The motion of particles from the outer magnetosphere toward low altitudes in the presence of the magnetospheric electric field produces an energy versus latitude dispersion that clearly identifies the cusp/cleft region. The low-latitude boundary of the magnetosheathlike particle precipitation marks a region referred to as the cleft and is often associated with the low-latitude boundary layer. The region of high-intensity precipitation just poleward of the cleft is the cusp proper. In regions poleward of the cusp, the intensity of the precipitation is reduced, and it has been inferred this is on field lines that map into the plasma mantle [*Rosenbauer et al.*, 1975]. The dayside extension of the boundary plasma sheet has also been identified in these low-altitude measurements. Using data from the Viking spacecraft, *Yamauchi and Lundin* [1993] have identified a new region at the poleward edge of the cusp/cleft region characterized by 100- to 300-eV field-aligned electrons. This region does not always occur when the interplanetary magnetic field is southward and never in the noon-midnight meridian.

Spacecraft measurements have provided evidence that magnetosheath plasma may cross the magnetopause both in regions where the magnetosphere is closed (i.e., the magnetospheric magnetic field lines are contained entirely within the magnetosphere) [e.g., *Eastman and Hones*, 1979], and where it is open (i.e., magnetospheric field lines extend from the Earth into interplanetary space) [e.g., *Hill and Reiff*, 1977]. In the case of magnetosheath plasma entry onto closed filed lines, some process such as plasma diffusion or anomalous transport due to waves must be involved. In the case of open magnetic field lines, the magnetosheath plasma is expected to have direct access into the magnetosphere, with some acceleration occurring at the magnetopause current sheet [*Speiser*, 1965; *Cowley*, 1980, 1982].

The energy-latitude dispersion of the precipitating cusp particles and the similarity of the particle flux to magnetosheath levels has led to the interpretation that the particle entry is occurring on open field lines [*Rosenbauer et al.*, 1975; *Reiff et al.*, 1977]. From observed V-shaped ion dispersion features, *Menietti and Burch* [1988] inferred that the region on the

Paper number 94JA02702.
0148-0227/95/94JA-02702$05.00

magnetopause surface across which magnetosheath particles are injected is only about 1 R_E wide. *Menietti and Smith* [1993] observed upward beams in the DE 1 data that suggest the presence of regions in which the energy dispersion appears to occur on both open and closed field lines. They suggested that the flux tubes that are associated with the dayside inverted Vs on closed field lines are in the process of becoming open. *Maynard et al.* [1991] examined data from both DE 1 and DE 2 during a magnetic storm in which DE 1 appears to have entered the magnetosheath. Twenty-two minutes before DE 1 crossed the magnetopause, DE 2 was in the southern cusp. The data were interpreted as being consistent with a cusp on open field lines and steady reconnection occurring at the magnetopause.

There are some features of the motion of the plasma particles that are injected across the magnetopause in the cusp region that are not fully understood. It has been shown [*Reiff et al.*, 1977] that we cannot simply map low-energy particle signatures along flux tubes back to the magnetopause because of electric field convection and the presence of strong inhomogeneities in the magnetic field. Because of the convection of open flux tubes, the particles observed at one low-altitude location and at one instant in time have crossed the magnetopause at a range of locations. For this reason, the identification of specific source regions based on the individual low-altitude spectra has recently been questioned [*Lockwood and Smith*, 1993; *Newell and Meng*, 1993]. *Sergeev and Bösinger* [1993] also showed how these effects can influence the association of low-altitude particle signatures with the open/closed field line boundary on the nightside. *Delcourt et al.* [1992] used particle simulations to show that ions can also suffer large modifications of their magnetic moments. This changes their mirror point and significantly alters their trajectories. The convection pattern of ions injected at the magnetopause also depends on the orientation of the interplanetary magnetic field (IMF). For a northward IMF, *Nishida et al.* [1993] showed from EXOS D (Akebono) measurements that poleward of the cusp an almost monoenergetic band of ions with energies of a few keV spanned several degrees in the polar cap.

The variations of particle signatures observed by satellites as they pass through the cusp and over the pole have also been interpreted in terms of temporal variations rather than spatial structure. *Lockwood and Smith* [1992] have shown that a model of a "pulsating" cusp is consistent with DMSP observations. This model has been used to estimate the variations in the reconnection rate from spacecraft data and to predict observable features at high and low altitudes resulting from time-dependent reconnection [*Lockwood and Smith*, 1994]. Analysis of ISEE 2 observations [*Phillips et al.*, 1993], however, have been interpreted in terms of a quasi-steady spatial structure and do not appear to be consistent with a brief, localized merging event.

In this paper, we present data from near-conjugate passes of the Dynamics Explorer 1 (DE 1), high altitude, and DE 2, low altitude, spacecraft [*Hoffman and Schmerling*, 1981] in the vicinity of the dayside cusp. We then compare the spacecraft measurements with three-dimensional model calculations of the expected particle precipitation at both spacecraft locations. The calculations are based on guiding center trajectories in steady state magnetospheric electric and magnetic fields and assume steady state reconnection at the dayside magnetopause. Under these assumptions, the entire magnetopause is open, allowing direct access of magnetosheath plasma into the magnetosphere at all locations on the magnetopause surface.

A similar model was previously used to compare calculated cusp particle spectra with data from a single pass of a DMSP spacecraft [*Onsager et al.*, 1993]. This earlier version of the model only considered particle motion in the noon-midnight plane and used a spatially uniform dawn-dusk electric field. The current model utilizes a three-dimensional magnetic field model and a dawn-dusk electric field that maps as expected for equipotential magnetic field lines.

The measurements from the high-altitude plasma instrument (HAPI) [*Burch et al.*, 1981] on DE 1 and the low-altitude plasma instrument (LAPI) [*Winningham et al.*, 1981] on DE 2 illustrate that a similar evolution in the electron and ion spectra was observed at two widely separated altitudes. In one of the cases analyzed, the observed ion dispersion was not smoothly varying with invariant latitude but rather a discontinuous jump in the ion energy occurred. The important aspect of this observation is that a similar, discontinuous ion dispersion signature was detected at both the high- and the low-altitude spacecraft, yet separated in universal time by about 20 min. This suggests that the discontinuity in the ion dispersion was due to spatial structure rather than temporal variations in the reconnection rate, and that reconnection had been occurring continuously for at least 20 min.

By comparing the observed electron and ion spectra with the model calculations, we demonstrate that measurements at both high and low altitudes can be modeled quantitatively by assuming steady reconnection at the dayside magnetopause. The observed spectra are consistent with the particle precipitation expected for magnetosheath electron and ion motion across an open magnetopause. In section 2, we present the ion and electron data from DE 1 at an altitude of approximately 3 R_E and from DE 2 at an altitude between approximately 500 and 800 km on September 27, 1981, day 81/270, and October 11, 1981, day 81/284, when the satellites are at about the same invariant latitude on the dayside near magnetic noon. In section 3, we describe the basic elements of the computational model. In section 4, the calculations are compared with the data. In section 5, the conclusions that can be drawn from the areas of agreement and disagreement are summarized.

2. Data

A conjugate pass of two satellites occurs when both are on the same field line at the same time. In this paper we present particle data in the Earth's magnetosphere from near-conjugate passes of DE 1 and DE 2 that provide information at different times and at different altitudes on field lines in the same magnetospheric region. We examine both electron and ion data at high altitude from HAPI on-board DE 1 and at low altitude from LAPI on-board DE 2. Both instruments are capable of detecting electrons and positive ions (assumed here to be protons) over the energy range from 5 eV to 32 keV and from 0° to 180° in pitch angle. We examine passes near magnetic local noon on day 81/270 and day 81/284, in which HAPI and LAPI measured particle precipitation that had the characteristics of magnetosheath electrons and ions. The cusp, polar cap, and the open/closed field line boundary at the two spacecraft positions are identified.

The DE 1 and the DE 2 orbits on day 81/270 plotted in the invariant latitude (IL) - magnetic local time (MLT) plane are shown in Figure 1. DE 1 passed through the dayside northern hemisphere between 11.4 and 12.7 MLT and DE 2 passed through this region between 12.0 and 13.9 MLT. Both spacecraft were traveling from low to high latitudes. An energy-time spectrogram of LAPI data from the first three intervals marked on the DE 2 orbit in Figure 1 is shown in the upper two panels

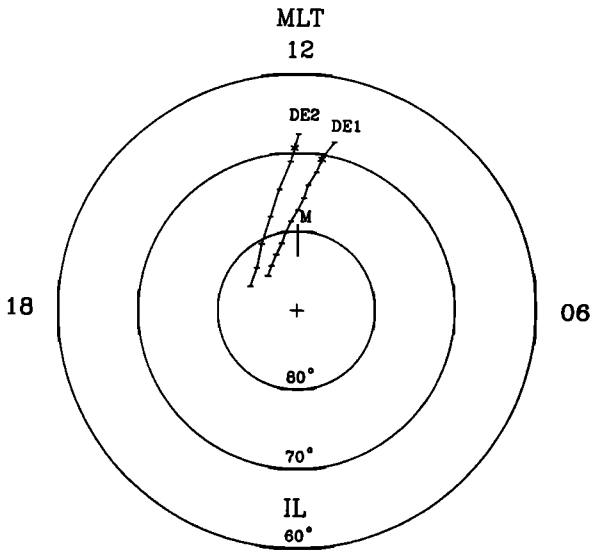

Figure 1. Orbits of DE 1 and DE 2 on 81/270 in the IL-MLT plane. Tick marks on the DE 1 orbit indicate 10-min intervals, on the DE 2 orbit 1 min intervals. The asterisk indicates where the spacecraft encountered the cusp. The line labelled by M shows the trajectory of the GSM z axis during the portion of the DE 1 orbit shown. The angle between the dipole axis (positive) and a point on this line gives the dipole tilt angle.

of Plate 1. The differential energy flux of the electrons (top panel) and the ions (second panel), both over energies from 5.1 eV to 27 keV, are plotted versus invariant latitude (IL) with the color scale indicating log differential energy flux from -5.9 to -2.5 ergs/(cm^2- s- sr- eV). The pitch angle of the electrons and ions is 14° - 16°.

As seen in the top panel, an energy flux enhancement of electrons with energy below about 400 eV occurred at 69.9° IL. The peak of the differential energy flux was as high as

4 x 10^{-3} ergs/(cm^2- s- sr- eV). There was another region of enhanced electron energy flux that began at 71.4° IL. The average energy and energy flux of the precipitating electrons then diminished as DE 2 moved further poleward. The precipitating ions with energy from 4 to 1 keV showed a pronounced energy flux enhancement that began at 70.2° IL. The ion energy and energy flux decreased with increasing latitude until a second intensity enhancement and increase in the maximum energy occurred at about 71.5° IL. The ion energy and flux then decreased again with increasing latitude.

In the second panel of Plate 1, the ion enhancement extending from 70.2° IL to 71.5° IL meets the total energy flux criterion of *Newell and Meng* [1988], i.e., it exceeds 10^{11} eV/(cm^2- s- sr), for identification of the low altitude cusp. The average energy of these ions is about 2 keV. The electrons in the same region, 69.9° IL to 71.4° IL, also had an energy flux greater than 10^{11} eV/(cm^2- s- sr), and they had an average energy below 200 eV. Therefore the electrons satisfy both the energy flux criterion and the average energy criterion of *Newell and Meng* [1988] for cusp precipitation. According to the National Space Science Data Center (NSSDC) OMNI database, the IMF was southward during this period. Under these conditions, the energy dispersion observed between 70.2° IL and 71.5° IL is a typical feature of cusp ions [*Rosenbauer et al.*, 1975; *Shelley et al.*, 1976; *Reiff et al.*, 1977].

The observed energy dispersion is referred to as the velocity filter effect [*Shelley et al.*, 1976] and is attributed to the dawn-dusk electric field causing a tailward $\boldsymbol{E} \times \boldsymbol{B}$ convection velocity. Because of the slower parallel speeds of the ions, the cusp ions appear later than the cusp electrons, and the low energy ions do not appear until the spacecraft moves further poleward, i.e., to higher latitudes. This characteristic cusp precipitation has been interpreted as being on newly opened field lines [*Rosenbauer et al.*, 1975; *Reiff et al.*, 1977; *Hill*, 1979; *Cowley et al.*, 1991], and a model incorporating this interpretation is presented in section 3. Thus the dayside open/closed field line boundary at 480 km and 12.1 MLT is interpreted to be located at 69.9° IL.

The second ion dispersion and the enhancement in the electron precipitation discussed above began at about 71.4° IL for the electrons and at about 71.5° IL for the ions, and it ended at approximately 72° IL in the electrons and perhaps at a little higher IL in the ions. On the basis of this data alone, this structural feature could be either temporal or spatial. We will see below that the DE 1 data support the interpretation that it is a spatial structure. Further poleward, beginning at approximately 74° IL, the ions disappeared and only low energy electron precipitation remained. This is the polar rain [*Winningham and Heikkila*, 1974] in the polar cap. The region between 72° IL and 74° IL is interpreted as the low-altitude extension of the plasma mantle.

Approximately 19 min later, DE 1 passed through the same region of the magnetosphere. An energy-time spectrogram of HAPI data covering the first six intervals of the DE 1 orbit plotted in Figure 1 is shown in the third and fourth panels of Plate 1. The pitch angle range of the observed electrons and ions is 7° to 17°, and the energy range is 5.9 eV to 13.2 keV. As shown in the third panel, DE 1 crossed a sharp boundary in the energy and the energy flux of the precipitating electrons at 71.1° IL. As shown in the fourth panel, HAPI began to measure intense energy flux of ions at 71.7° IL. The energy and the energy flux of this enhanced precipitation are again typical of magnetosheath particles. The characteristic cusp energy dispersion of the ions was also present. Therefore DE 1 also encountered the cusp. On the basis of the low-latitude edge of the cusp precipitation, the dayside open/closed field line boundary at 18,600 km altitude and 11.4 MLT is interpreted to be located at 71.1° IL.

Just as in the DE 2 data, there was a break in the ion energy dispersion and then the commencement of a second ion dispersion event that began at 73.0° IL and extended to approximately 74.1° IL. The electron data from DE 1 showed only a weak indication of the second event. The region between 74° IL and 76° IL is presumably the mantle. Again, polar rain electrons were detected in the polar cap poleward of approximately 76° IL.

The equatorward boundary of the cusp observed on the two spacecraft differs by about 1.2° IL. This may be due to either temporal variation of the cusp features between the time of the two spacecraft passes or the different magnetic local times of the events. As shown in Figure 1, DE 1 and DE 2 are not in perfect conjunction. DE 1 passed the cusp just before magnetic noon, while 19 min later, DE 2 passed the cusp just past magnetic noon.

The important point we stress with regard to the observations on day 81/270 is that both the high-altitude and the low-altitude spacecraft detected two similar, distinctive ion dispersion structures at nearly the same invariant latitude and magnetic local time, yet separated in universal time by approximately 20 min. This indicates that the ion dispersion signature was a spatial structure rather than a temporal feature. Furthermore, this spatial feature appears to have persisted for at least 20 min.

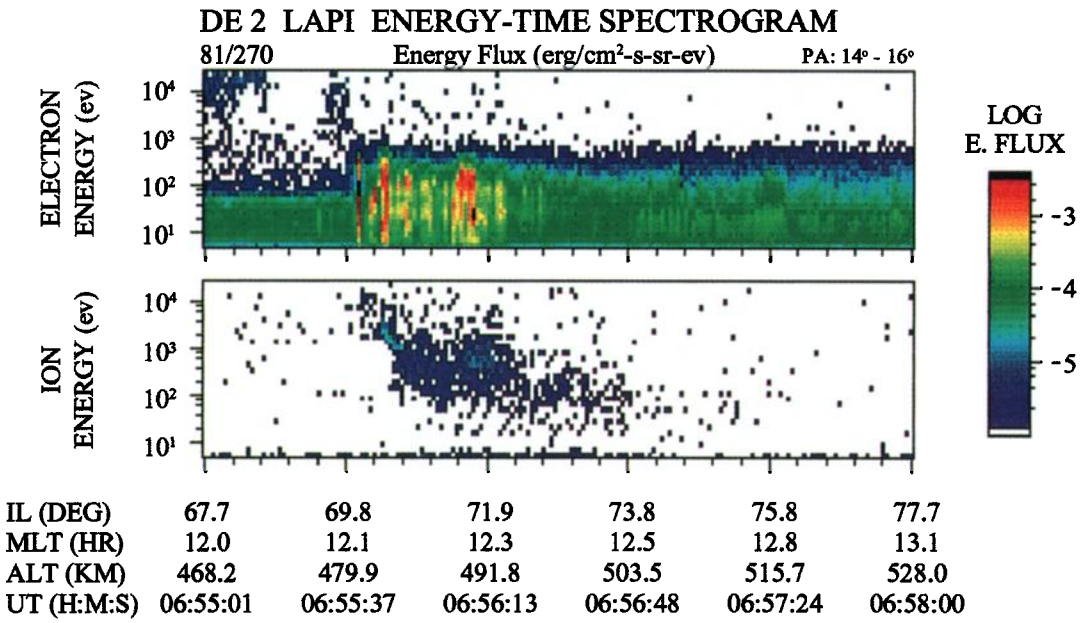

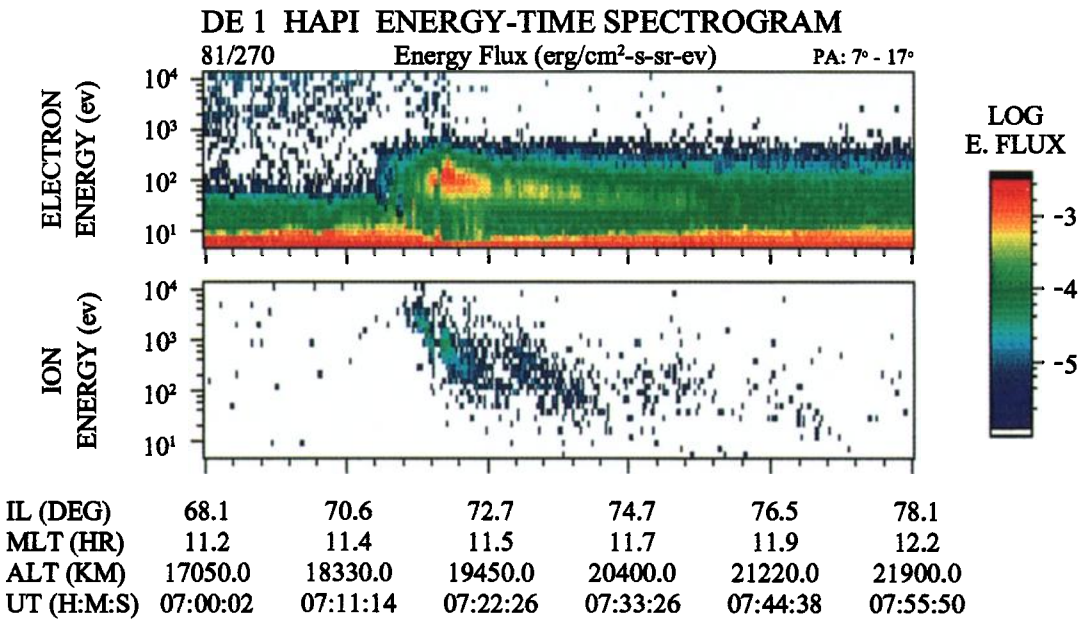

Plate 1. Measurements from the low-altitude DE 2 spacecraft (upper panels) and the high-altitude DE 1 spacecraft (lower panels) of electron and ion precipitation during near-conjugate traversals of the cusp. Both spacecraft detected two distinct ion dispersion signatures at about the same invariant latitude, yet separated in universal time by more than 20 min. The discontinuous ion dispersion signatures are interpreted as being due to a spatial structure rather than a temporal variability in the reconnection rate.

On day 81/284, another near conjugate event of DE 1 and DE 2 was observed. The orbits are shown in Figure 2 in the same format as Figure 1. The NSSDC OMNI database shows that the interplanetary magnetic field had a southward component prior to and during these measurements. The top two panels in Plate 2 show the energy spectrogram for the first three intervals in the DE 2 orbit shown in Figure 2. The energy range for the spectrogram is the same as for 81/270, and the pitch angle range is 14° - 20°. LAPI observed an enhanced energy flux of electrons beginning at 70.0° IL. An intense flux of ions with energy dispersion began at 70.4° IL and ended at approximately 71.4° IL. This region that is traversed by DE 2 in 15 s is identified as the cusp based on the definition of *Newell and Meng* [1988]. Poleward of the cusp, the average energy and the energy flux of the ions decreased gradually while the energy dispersion of the ions continued. These ions are believed to be mantle precipitation; i.e., they are likely to be on field lines that now penetrate the magnetopause on the nightside. This DE 2 pass is a typical cusp/mantle crossing near magnetic local noon. The spacecraft is interpreted as crossing the open/closed field line boundary at

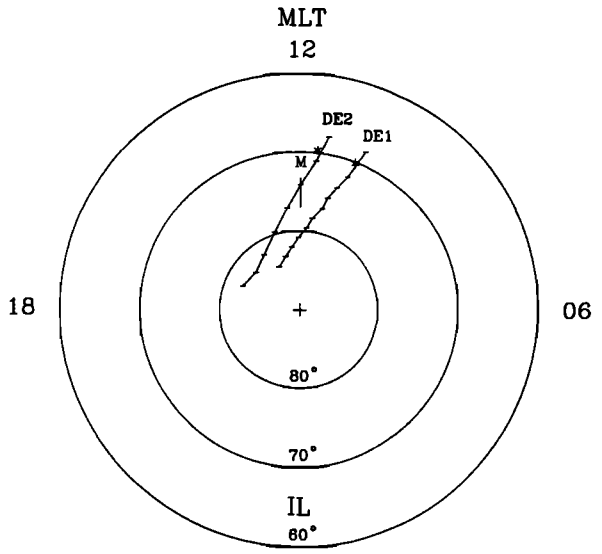

Figure 2. Orbits of DE 1 and DE 2 on 81/284 in the IL-MLT plane. The format is the same as Figure 1.

70.2° IL, 11.6 MLT, and 746 km. No second ion dispersion or electron enhancement event was observed on this day.

At high altitude on day 81/284, approximately 10 min later, DE 1 passed through the same region. The third and fourth panels of Plate 2 present an energy spectrogram of data from the first seven intervals of the orbit shown in Figure 2. The pitch angle range is 4° to 24°, and the energy range is 4.5 eV to 17.5 keV. The energy flux enhancement of electrons began at 70.7° IL as shown in the third panel. The enhancement and dispersion of precipitating ions occurred 96 seconds later at 71.0° IL, shown in the fourth panel. The average energy and energy flux of these electrons and ions are values typical of magnetosheath particles. As the spacecraft moved to higher latitude, the ion energy and flux continued to decrease. In addition, there was an extended region in which there was a weak ion flux that had an almost constant energy of approximately 100 eV. Also, in contrast to 81/270, the peak electron and ion flux at DE 2 was about an order of magnitude higher than that observed at DE 1. A possible explanation is suggested in Figure 2 where we see that on 81/284, DE 2 encountered the cusp very near magnetic noon whereas DE 1 was about 1 hour toward the morningside. Since both spacecraft saw regions of similar particle precipitation with boundaries separated by only 0.7° IL and approximately 10 min UT, the data again suggest that there are quasi-stationary structures in the cusp/cleft region of the magnetosphere.

3. Model Description

The high- and low-altitude particle measurements described above have been modeled using a three-dimensional steady state description of particle transport from the solar wind to spacecraft locations in the magnetosphere. With this model we are able to estimate the electron and ion distribution functions on open field lines by specifying solar wind parameters and by making various assumptions about the magnetospheric electric and magnetic fields and the particle transport across the magnetopause current sheet. In addition, we calculate the locations where particles detected within the magnetosphere have crossed the magnetopause surface.

For these calculations we assume that steady state reconnection is occurring at the subsolar magnetopause, so that the entire dayside magnetopause is open to magnetosheath plasma entry. At a given spacecraft location on open field lines in the magnetosphere, the positions along the magnetopause from which the particles have arrived is determined by the velocity filter effect [*Rosenbauer et al.*, 1975]. As particles move along the magnetic field from the magnetopause, they simultaneously $\boldsymbol{E} \times \boldsymbol{B}$ drift perpendicular to it. Particles with parallel speeds much higher than the $\boldsymbol{E} \times \boldsymbol{B}$ drift speed will drift only a small distance perpendicular to the magnetic field in the time required to move the parallel distance to the spacecraft. Particles with lower parallel speeds will undergo a larger drift perpendicular to the field in the time required to reach the spacecraft from the magnetopause. As a result of this velocity filter effect, there is a one-to-one correspondence between the parallel speeds of particles detected at a given spacecraft location and the locations along the magnetopause where the particles originated.

The mapping used to calculate the electron and ion spectra is done in three stages [*Onsager et al.*, 1993]. First, we use the discrete energies and pitch angles that the spacecraft particle detectors measure and follow the corresponding particle trajectories backward in time from locations along the spacecraft trajectory to the magnetopause. The model spectra presented in this paper have been produced using 31 logarithmically spaced energy steps ranging from 5 eV to 27 keV, corresponding approximately to the discrete energies measured by LAPI (Plates 1 and 2). With the magnetic field model described below, the magnetopause is defined to be a paraboloid of rotation, with a subsolar location of $x_{gsm} = 10\ R_E$ and a radial distance of $15\ R_E$ in the day-night terminator plane. The particle trajectory calculations are interrupted when the magnetopause surface is reached. From this stage of the calculation we obtain the locations along the inner surface of the magnetopause from which particles detected at a given location in the magnetosphere have originated.

The particle motion is determined using prescribed magnetospheric electric and magnetic fields. We numerically integrate the guiding center position and velocity including only the mirror force in the parallel equation of motion. We assume that the magnetic moment is conserved along the particle trajectory. Other sources of parallel acceleration such as those due to centrifugal and Coriolis-like effects [e.g., *Mauk and Meng*, 1991] are expected to have a minor influence on the particle motion for the parameters used in the model calculations (see section 4) and therefore have not been included. For example, analysis of low energy particle data from DE 1 at mid altitudes on the nightside [*Liu et al.*, 1994] showed that centrifugal acceleration could produce parallel energies of the order of tens of electron volts but only with an electric field many times larger than the one used in the calculations reported here.

We have used the *Stern* [1985] magnetic field model to approximate the field within the magnetosphere. This field model in its simplest form gives a closed magnetosphere by using a parabolic magnetopause current sheet to shield the Earth's dipole field. We have used a tilted dipole axis appropriate for the time of the measurements, with a tilt of -10.5° on day 81/270 and -16.5° on day 81/284. The tilt is about the y_{gsm} direction, with negative angles corresponding to northern hemisphere winter.

We then superimpose a spatially uniform, southward magnetic field ($-z_{gsm}$) with a magnitude of 2 nT to obtain an open magnetic field configuration. This southward magnetic field has been added only to provide a normal component of the field across the magnetopause. In reality, the draping of the magnetosheath field will produce substantial x and y components of the

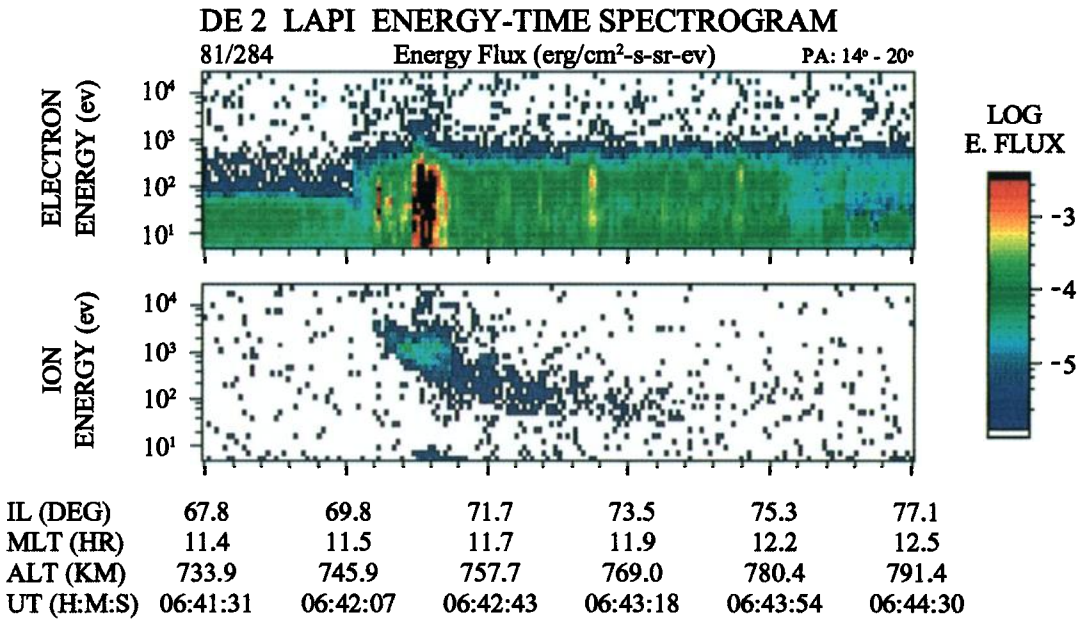

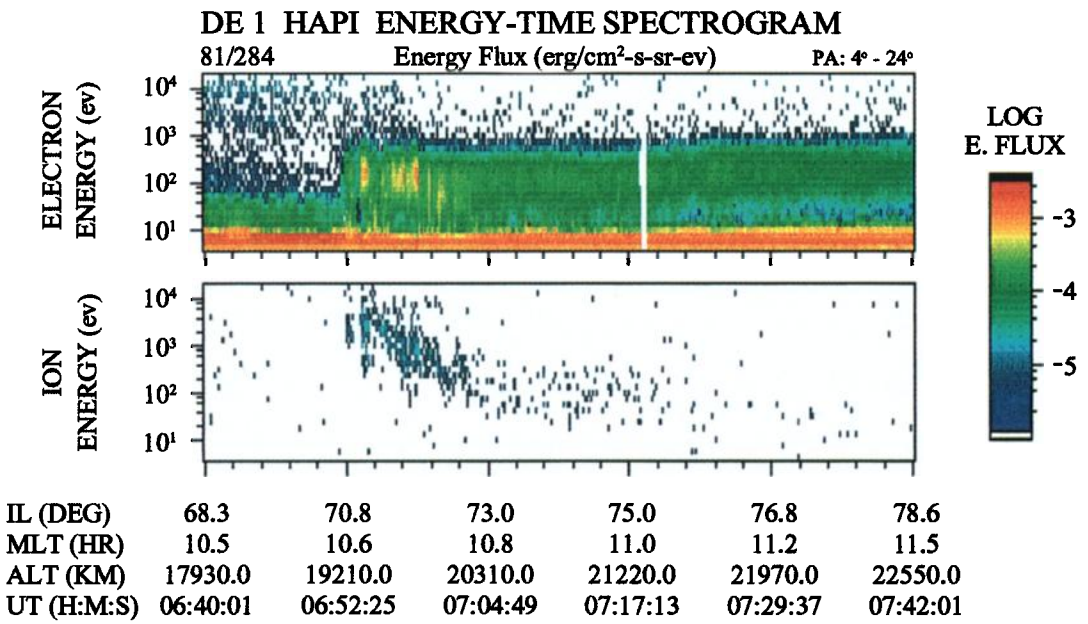

Plate 2. Measurements from the low-altitude DE 2 spacecraft (upper panels) and the high-altitude DE 1 spacecraft (lower panels) of electron and ion precipitation during near-conjugate traversals of the cusp. Both spacecraft detected similar ion dispersion signatures at about the same invariant latitude.

field in the magnetosheath, and some small fraction of this field will penetrate across the open magnetopause. Since we have not modeled the actual orientation of the magnetosheath field, nor do we know the fraction of this field that will penetrate across the magnetopause, we have simply superimposed a southward directed field to produce an open magnetosphere. From the model calculations, we have found that the magnitude of the normal component of the magnetic field influences the width of the cusp ion spectra in both energy and in latitude. A superimposed southward field of 2 nT resulted in model spectra that approximately match the measured spectra.

The electric field used in the particle trajectory calculations is obtained by specifying a value for the electric field at the ionosphere and then by scaling it as the square root of the magnetic field magnitude, as would be the case for equipotential magnetic field lines. We take this field to be in the $+y_{gsm}$ direction, i.e., dawn-to-dusk. Although the magnetic field model we have used is three dimensional, the choice of a strictly dawn-to-dusk electric field causes the $\boldsymbol{E} \times \boldsymbol{B}$ drift to be confined to the x-z plane. Representative particle trajectories were illustrated by *Onsager et al.* [1993] where Figure 1 shows clearly how particles of different energy observed by a satellite come from different positions on the magnetopause.

The second stage of the mapping is to calculate the particle velocities on the outer surface of the magnetopause such that when the particles cross the magnetopause they obtain the

velocities on the inner surface that resulted from the first stage of the mapping. This calculation first involves the transformation into a de Hoffman-Teller reference frame, i.e., the frame moving along the magnetopause in which the convection electric field is zero. [*Hill and Reiff*, 1977; *Cowley*, 1980, 1982]. We determine the speed of this reference frame from the requirement that in this frame, the magnetosheath bulk flow is magnetic field aligned at the magnetosheath Alfven speed [e.g., *Cowley and Owen*, 1989],

$$\vec{V}_f = \vec{V}_{sh} - V_A \hat{b}_{sh} \quad , \tag{1}$$

where $\vec{V}_f$ is the de Hoffman-Teller frame velocity, $\vec{V}_{sh}$ is the magnetosheath flow velocity, $\vec{V}_A$ is the magnetosheath Alfven speed, and $\hat{b}_{sh}$ is a unit vector in the direction of the magnetosheath magnetic field.

In general, the magnetosheath flow velocity and the magnetic field will have components normal and tangent to the local magnetopause,

$$\begin{aligned} \vec{V}_{sh} &= V_n \hat{n} + V_t \hat{t}_f \\ \hat{b}_{sh} &= b_n \hat{n} + b_t \hat{t}_b \end{aligned} \quad , \tag{2}$$

where $\hat{t}_f$ and $\hat{t}_b$ are unit vectors in the directions of the tangential plasma flow and the tangential component of the magnetic field, respectively, and $\hat{n}$ is the local unit normal to the magnetopause. The local normal direction and the tangent plane are determined from the parabolic surface used in the magnetic field model [*Stern*, 1985]. With the requirement that the de Hoffman-Teller frame velocity be tangent to the magnetopause, (1) becomes

$$\vec{V}_f = \vec{V}_t \hat{t}_f - V_A b_t \hat{t}_b \quad , \tag{3}$$

with the additional condition

$$V_n = V_A b_n \quad . \tag{4}$$

For the examples discussed here, we have taken the magnetosheath magnetic field to lie in the $(-z_{gsm})$ direction, and we have assumed that the flow velocity diverges away from the subsolar point. We have used the magnetosheath flow speed obtained from gas-dynamic calculations (described below) as the total flow speed, $|\vec{V}_{sh}|$, and then determined the tangential flow velocity by subtracting off the normal component, as given by (4). Nearly identical results are obtained when the flow speed determined from gas-dynamic calculations is taken to be the tangential flow speed, V_t, rather than the total speed.

We assume that in this reference frame, the particle energy and pitch angle are conserved on crossing the magnetopause. With these assumptions, the change in velocity across the current sheet corresponds to a rotation of the velocity vector in this reference frame by an angle given by the rotation in the magnetic field. Finally, the velocity is transformed back to the spacecraft reference frame. This stage of the calculation yields the particle velocities and locations along the outer surface of the magnetopause that particles detected at the specified location in the magnetosphere would have had.

An important aspect of these calculations is that we follow only guiding center trajectories, and therefore, specifically disallow any gyrophase dependence of the particle trajectories. In this way, we are calculating the trajectories of volume elements in phase space, rather than individual particles. It is true that individual particle trajectories may undergo non-adiabatic transitions at the current sheet and in the low magnetic field region of the high altitude cusp [e.g., *Delcourt et al.*, 1992]. The intent in this model is to determine what features of the observations can be explained in terms of adiabatic motion. One advantage to associating the calculated guiding center trajectories with phase space trajectories is that Liouville's theorem can be used to quantitatively estimate phase space density from a single trajectory, rather than needing to accumulate large numbers of particle trajectories to estimate particle properties statistically.

The final stage of the mapping is to determine the values of phase space density at the spacecraft location from the magnetosheath properties. The magnetosheath plasma density, temperature, bulk flow speed, and the magnetic field magnitude are estimated from the results of gas-dynamic and convected magnetic field calculations [*Spreiter and Stahara*, 1985, Figures 10 and 12]. The polynomial fits we have produced from the gas-dynamic results are shown in Figure 3. From top to bottom the panels contain the density, temperature, bulk flow speed, and the magnetic field magnitude as a function of x_{gsm} along the outer surface of the magnetopause. The magnetic field magnitude is used to calculate the Alfven speed, which is needed to determine the de Hoffman-Teller frame speed as described above. All values are normalized to the asymptotic solar wind values.

For the calculations described below, we use measured or assumed solar wind parameters and the polynomial fits shown in Figure 3 to determine the magnetosheath parameters at any location along the magnetopause. We take the magnetosheath electron and ion distributions to be flowing Maxwellians. By assuming that phase space density is conserved along the particle trajectories, we assign the values of phase space density at the locations in the magnetosheath where the particles originated to the specified spacecraft locations in the magnetosphere where the particles would be detected. In addition, we allow for the reflection of a fraction of the incident magnetosheath particles at the magnetopause and investigate the necessary reflection coefficient required to match the model results with the observations.

4. Model Results

The model results calculated along the trajectories of the DE 1 and the DE 2 spacecraft on day 81/270 are shown in Plate 3, using the same format as Plate 1. The model results cover a range of approximately 10° IL, similar to the data described above. Since we have only modeled the entering magnetosheath plasma, there is no particle flux in the closed field line region, which in this case is below about 80° IL.

The parameters we have used for the calculations shown in Plate 3 are listed in Table 1. The values chosen for the solar wind parameters (top five items in Table 1) are based on 1-hour averages from the NSSDC OMNI data. The measured values from hour 7 on day 81/270 are a density of 7.1 cm^{-3}, an ion temperature of 4.6×10^4 K, a bulk flow of 419 km/s, magnetic field components of {-4.2, 0.5, -5.4} nT in GSM coordinates, and a magnetic field magnitude of 7.4 nT. The measured solar wind magnetic field magnitude is used in conjunction with the bottom panel of Figure 3 to calculate the Alfven speed in the magnetosheath at any location along the outer surface of the magnetopause. The average values varied considerably from

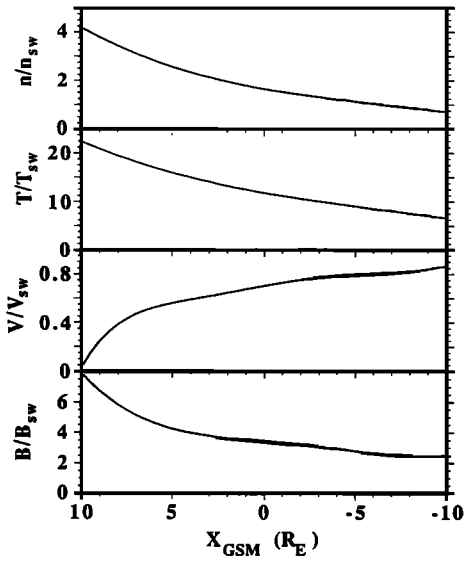

Figure 3. Polynomial fits to thegas-dynamic results of *Spreiter and Stahara* [1985] for the magnetosheath density, temperature, velocity, and magnetic field as a function of the x_{gsm} coordinate along the magnetopause.

hour to hour and are only taken as an approximate indication of the solar wind properties.

In addition to the solar wind parameters, we have specified the dawn-dusk electric field (in terms of the ionospheric convection velocity) and the particle reflection coefficients at the magnetopause. The electric field is specified in terms of the ***E x B*** drift speed at the location of DE 2. An ***E x B*** drift speed of 125 m/s corresponds to an electric field of approximately 6 mV/m at DE 2, where the magnetic field magnitude is about 47,000 nT. The electric field at DE 1 is approximately a factor of 8 smaller, scaled by the square root of the ratio of the magnetic field strengths at the two spacecraft.

One difference between the calculated and the measured spectra is the location of the cusp. The low-latitude edge of the measured cusp electron and ion signatures, interpreted as the open/closed field line boundary, is located at approximately 70° IL (Plate 1), whereas the model places this boundary at about 80° IL. The cusp location in our calculated spectra is also approximately two or three degrees higher in latitude than the average cusp location determined from DMSP data [*Newell and Meng*, 1992]. For the model results described here, we have not included a ring current nor have we reduced the magnetopause current to allow for leakage of the Earth's dipole field out of the magnetosphere as provided for in the *Stern* [1985] model to reduce the latitude of the cusp. We have chosen to use a relatively simple form of the magnetic field model and concentrate primarily on the variation in the cusp particles with latitude, rather than on the absolute location of the cusp. The position of the measured cusp particles at latitudes well below the average location is perhaps due to an erosion of the dayside magnetic flux associated with a southward interplanetary magnetic field [e.g., *Burch*, 1972]. This effect has not been included in the model presented here.

The electron and ion spectra calculated with the model show the same general trends and similar flux levels as the spacecraft measurements. As with the data, the model spectra are the most intense and extend to the highest energies at low latitudes. The flux intensity and the energy of the precipitating particles then decrease with increasing latitude. Note also that all the color scales used to represent the calculations and the measurements are identical.

The energy-latitude dependence and the flux levels of the model spectra are controlled by various features of the model. The agreement between the calculated slope of the minimum ion energy with latitude and the observed slope is determined primarily by the magnitude of the dawn-to-dusk electric field. Larger electric field values result in a smaller slope. This results from the velocity filter effect; as particles flow from the magnetopause toward the Earth, they ***E x B*** drift perpendicular to the field. The latitudinal separation of the particles due to their different travel times from the magnetopause to the spacecraft will be greater for a larger electric field. Spectra were calculated using various values of the electric field, and the electric field used in the calculations shown here was chosen to match the slope of the observed ion dispersion.

The variation in the average ion energy with latitude and the overall width of the ion dispersion in energy and in latitude are well reproduced by the model. The model produces a single ion spectrum rather than the two dispersion features seen in the spacecraft data. As described above, we attribute the two dispersion features to a spatial structure, perhaps involving two reconnection lines, that both spacecraft pass through. Since the model includes only a single reconnection line, we only reproduce the first of the two dispersion features.

As given in Table 1, we have used separate electron and ion temperatures for the model calculations. The NSSDC OMNI database, however, only provides the ion temperature. In addition, the gas-dynamic calculations used to estimate the magnetosheath properties contain only a single fluid, and therefore do not account for the difference in the electron and ion heating at the bow shock. Because of these uncertainties, the electron and the ion temperatures used for the model calculations have been adjusted independently to provide the best fit to the data, rather than simply using the single, measured value.

The electron temperature was chosen to match approximately the modeled and the observed energy at which the maximum electron flux occurred. This can be seen as the red-yellow region in the spectra occurring at about 100 eV near the low-latitude edge of the dispersion signature (for example, 79.8° - 80.8° IL in the model DE 1 spectrum). The yellow region obtained in the model is somewhat broader than in the data, yet the overall structure is similar. The model electron temperature which produces this approximate match to the data is slightly below the measured (1-hour average) temperature. The ion temperature was taken to be a factor of 5 larger than the electron temperature, consistent with magnetosheath observations. This ion temperature results in model spectra that match reasonably well the measured spectral width and the energy of the peak ion fluxes.

The overall flux levels in the calculations are controlled by the input solar wind density and by an assumed reflection coefficient at the magnetopause. We have used model densities that approximately equal the measured solar wind values. Therefore the only remaining parameter to adjust the model flux levels is a reflection coefficient. A reflection coefficient of zero corresponds to the case where all magnetosheath particles incident on the magnetopause would enter the magnetosphere along all open field lines.

The reflection coefficient used to model the DE 1 electron measurements on 81/270 is 0.2; i.e., 80% of the electrons incident on the magnetopause freely enter the magnetosphere. On the other hand, the ion reflection coefficient needed to match the ion observations is 0.9, i.e., only 10% of the ions enter the

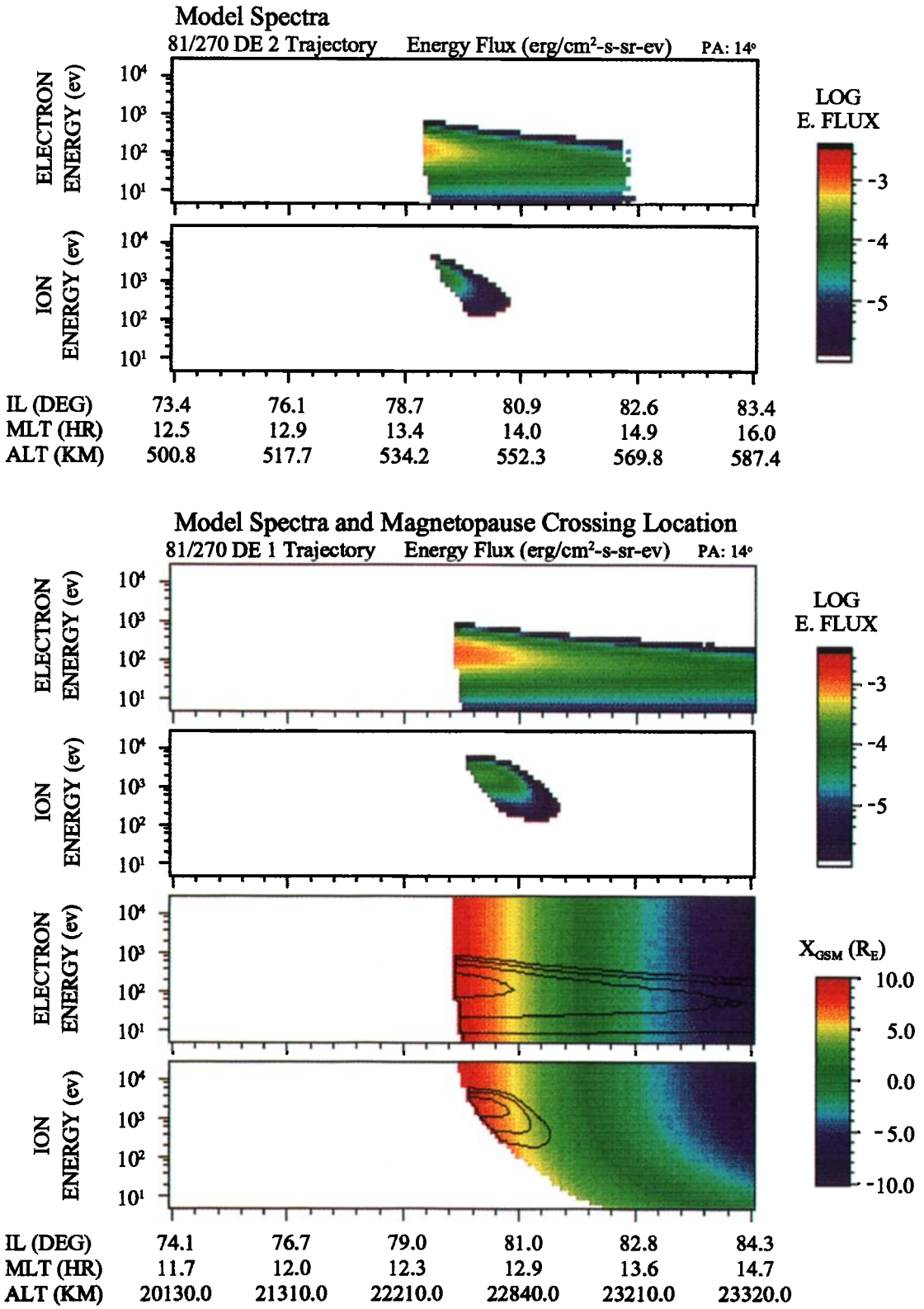

Plate 3. Model calculations of the cusp electron and ion spectra for day 81/270. In the upper two panels the DE 2 spacecraft trajectory is used. In the middle two panels, the DE 1 trajectory is used. These spectra match closely the measured spectra shown in Plate 1. The lower two panels show the x_{GSM} source location of the particles (as indicated by the color scale) and the particle flux levels along the model DE 1 trajectory (as indicated by the contour lines).

Table 1. List of Model Parameters Used in Calculations to be Compared With Data

Model Parameter	Day 81/270	Day 81/284
Solar wind density	7 cm^{-3}	16 cm^{-3}
Solar wind electron temperature	4.0 x 10^4 K	4.0 x 10^4 K
Solar wind ion temperature	2.0 x 10^5 K	4.0 x 10^5 K
Solar wind velocity	420 km/s	450 km/s
Interplanetary magnetic field	7 nT	10 nT
Ionospheric convection velocity	125 m/s	500 m/s
Dipole tilt	-10.5°	-16.5°
Electron reflection coefficient	0.2	0.2
Ion reflection coefficient	0.9	0.9

magnetosphere. At present, the reason for this large reflection coefficient and the difference between the electron and ion coefficients is not clear. It is, of course, the case that quasi-neutrality must be preserved in the plasma. Any difference in the densities of the entering magnetosheath electrons and ions can, in principle, be compensated by a difference in the ionospheric and magnetospheric plasma components [*Burch*, 1985], which are not modeled here.

For these calculations, we have used the same parameters for both the DE 1 and DE 2 trajectories. As can be seen by comparing with Plate 1, the calculated spectra match the measurements quite well. Although the observed short timescale bursts of electrons are not reproduced by the model, the overall shape and flux levels of the electron spectra are similar to the observations. The abrupt high latitude edge of the model electron spectra is due to the fact that we have truncated our results at x_{gsm} = -10 R_E. Since the *Stern* [1985] field model does not have a magnetotail current, the model field becomes less accurate with increasing downtail distance. We have only calculated spectra for particles that encounter the magnetopause sunward of x_{gsm} = -10 R_E.

An important result of this comparison of DE 1 and DE 2 calculated spectra is that the same model parameters successfully reproduce the measurements at both spacecraft. These model parameters include the measured solar wind properties, the ionospheric convection electric field, and the reflection coefficients at the magnetopause. This indicates that the calculational techniques employed here are valid at both high and low altitudes and are likely to be applicable over large areas of the open field line region. Since the DE 1 and the DE 2 spacecraft detected the cusp precipitation separated by approximately a half hour in universal time, the agreement at both spacecraft with the steady state model suggests that reconnection was occurring on a steady basis for at least about one half hour.

Another application of our model is to investigate the locations along the magnetopause surface where particles detected within the magnetosphere have originated. The magnetopause crossing points of the model particles for the DE 1 trajectory on day 81/270 are illustrated in the bottom two panels of Plate 3. The ion and electron spectra are indicated by the solid black contours. These contours represent the same information as is shown in the third and fourth panels of Plate 3. The x_{gsm} coordinate of the point where the model particles have crossed the magnetopause surface is indicated by the various colors. The white regions indicate the energies and the latitudes where the detected particles have originated on closed magnetic field lines.

The open/closed field line boundary can be identified in the bottom panel of Plate 3 as approximately the location where the highest-energy electrons are first detected, at about 79.4° IL. The velocity filter effect can be clearly seen by the energy-latitude slope in the source location of the ions. This slope is not as evident in the electron plot, since even the lowest-energy electrons shown have speeds far in excess of the $\boldsymbol{E} \times \boldsymbol{B}$ drift speed.

It is also clear from the bottom panel of Plate 3 that the calculated ions with observable fluxes come from a fairly narrow range of energies and latitudes at the magnetopause. Although particles from the magnetosheath have access to the spacecraft over a broad latitude and energy range, the fluxes of particles at those locations in the magnetosheath may be below the detection threshold of the instrument. At any given latitude, the ions that comprise the observed spectrum have come from a region on the magnetopause surface that is about 1 - 2 R_E in extent, similar to earlier estimates based on DE 1 data by *Menietti and Burch* [1988], but the width of the observed ion spectra in energy or latitude does not necessarily give any information about the spatial extent of the open region on the magnetopause as postulated by *Menietti and Burch* [1988]. The decrease in precipitating flux with increasing latitude is due largely to the changes in the magnetosheath properties with position away from the subsolar point, i.e., decreasing density, decreasing temperature, and increasing tailward bulk flow (see Figure 3). Even with free access of the magnetosheath particles across the entire magnetopause, the spectra detected at a spacecraft within the magnetosphere can be quite narrow in energy and in latitude.

The model calculations of the DE 1 and the DE 2 spectra using the spacecraft trajectories on day 81/284 are shown in Plate 4. These calculations are to be compared with the measurements shown in Plate 2. The parameters we have used for these calculations are given in Table 1. The measured solar wind properties obtained from the NSSDC OMNI database for hour 6 of day 81/284 are a density of 16 cm^{-3}, a bulk flow of 454 km/s, magnetic field components of {2.7, 7.0, -5.4} nT, and a magnitude of 9.5 nT. The ion temperature was not available at this time.

As for 81/270, the model electron and ion spectra for 81/284 match the observations reasonably well. Many of the short time-scale variations in the measurements are not reproduced by the model; however, the overall energy-latitude slope of the ion spectra and the average electron and ion flux levels are fairly well matched. The open/closed field line boundary, as inferred from the onset of the cusp electrons and ions, is approximately 10° IL higher in the model than in the observations. This difference presumably is due to the magnetic field model we have used, as discussed above.

The difference in the cusp location in the model from its observed location has other noticeable effects on the calculated spectra. Because the spacecraft trajectories vary in local time as well as in latitude (Figure 2), the model cusp ion and electron precipitation are found at different local times than the observa-

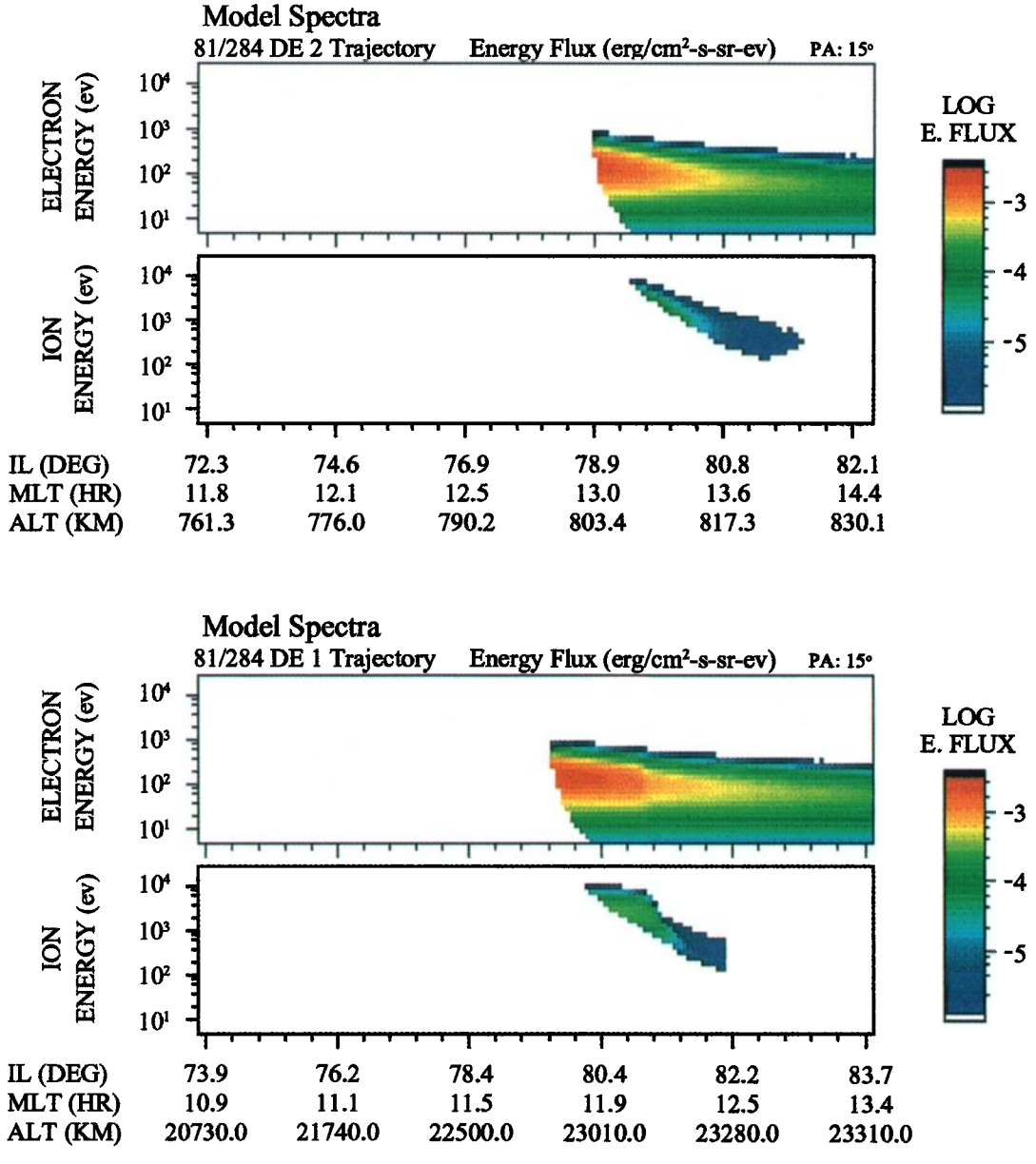

Plate 4. Model calculations of the cusp electron and ion spectra for day 81/284. In the upper two panels the DE 2 spacecraft trajectory is used. In the middle two panels, the DE 1 trajectory is used. These spectra match closely the measured spectra shown in Plate 2.

tions. For example, the DE 1 cusp particles (lower panels of Plate 2) are detected at about 10.7 MLT, while the model cusp particles are centered around 12 MLT. Since the model cusp is located closer to noon, and therefore maps closer to the subsolar point than the observed cusp particles, we expect the model fluxes to be somewhat higher than the observed fluxes.

On the other hand, the cusp precipitation measured by DE 2 (upper panels of Plate 2) occurred at approximately 11.6 MLT, while the calculated cusp spectra, which occur at a higher latitude portion of the DE 2 trajectory, were centered around 13.6 MLT. For this reason, it is understandable that the calculated ion spectra are not as broad in energy as the observed spectra, particularly at the low-latitude edge of the cusp precipitation where the most intense fluxes are typically observed. Namely, since the particles detected away from noon map to magnetosheath locations farther from the subsolar point, the spectra observed there will reflect the cooler, less dense properties of the source population.

5. Discussion and Summary

In this paper we have presented data and model calculations of magnetosheath plasma at both high and low altitudes in the dayside magnetosphere. Data from two near-conjugate passes of the DE 1 and the DE 2 spacecraft through the cusp region have been shown. These data exhibit the typical electron and ion properties observed in the cusp, i.e., magnetosheathlike flux levels and velocity dispersion [*Reiff et al.*, 1977]. In both cases, the interplanetary magnetic field was directed primarily southward, and the observed ion dispersion was consistent with the presence of a dawn-dusk directed magnetospheric electric field. The two spacecraft both detected the cusp particle precipitation

at approximately the same invariant latitude and magnetic local time, but the universal time at which the cusp particles were detected differed by approximately 20 min in one case and approximately 10 min in the other case.

During the cusp crossing on September 27, 1981, day 81/270, both spacecraft detected first a gradual decline in ion energy with increasing latitude, then an abrupt upward step in the ion energy, followed by a second gradual decline in energy. As has been demonstrated recently [*Lockwood and Smith*, 1992, 1994], a temporal variation in the reconnection rate at the magnetopause can create abrupt jumps in the observed ion energy in the cusp. From analysis of data from a single spacecraft (either DE 1 or DE 2), one might conclude that the observed ion signature was due to such a temporal variation in the reconnection rate. In the example presented here, however, both spacecraft detect similar ion dispersion signatures at approximately the same invariant latitude and magnetic local time, yet separated by approximately 20 min in universal time. We interpret the similar ion signatures at the two spacecraft to be due to quasi-steady spatial variations, rather than to temporal variations in magnetopause reconnection.

From a model based on magnetosheath transport across the open magnetic field regions of the magnetopause [*Onsager et al.*, 1993], we have calculated the electron and ion spectra at both the high- and the low-altitude spacecraft locations and compared them with the data. The calculated electron and ion spectra are found to exhibit the same general cusp structure as found in the data. Since the model calculations include only particles entering the magnetosphere on open magnetic field lines, the similarity between the model results and the data suggests that the observed cusp particles are detected on open field lines. No magnetosheath entry onto closed field lines is required to account for the observed particle spectra in these cases.

These calculations have used the measured solar wind properties as input parameters. In order to further match the calculated and the observed fluxes, we have specified independent solar wind electron and ion temperatures and electron and ion reflection coefficients at the magnetopause. The dawn-dusk electric field has been chosen to match the energy-latitude slope of the ion dispersion. One important result of these comparisons with DE 1 and DE 2 conjunctions is that the same model parameters can successfully match the spectra at both spacecraft. This result indicates that the modeling technique employed here is applicable at both high and low altitudes. Also, since the DE 1 and the DE 2 cusp spectra are not detected simultaneously but rather were separated in universal time by 10 - 20 min, this ability to model the observations at both spacecraft using the same parameters suggests that the magnetospheric and magnetosheath conditions affecting the cusp precipitation were not changing appreciably on this time scale. This indicates that quasi-steady reconnection was probably occurring at these times.

Another result of the model is the estimation of the magnetopause crossing points of the precipitating electrons and ions. We have found that at any given spacecraft location, the electrons and ions have come from a fairly narrow spatial region on the magnetopause, spanning roughly 1 to 2 R_E. This spatial region is of approximately the same size as that of previous estimates [*Menietti and Burch*, 1988]. The width of the ion spectrum at a given latitude and pitch angle was interpreted by these authors as resulting from a spatially limited ion injection region. This ion injection region was attributed to a latitudinally narrow region of magnetic merging, with a size on the order of that estimated for FTEs. The important result shown here is that the modeled ion spectra have a width consistent with the observations, even though magnetosheath plasma has access to the magnetosphere over the entire magnetopause. The properties of the ion spectra depend on a number of factors, such as the magnetosheath properties, the de Hoffman-Teller frame speed, and the magnetic field rotation at the magnetopause, which vary continuously away from the subsolar point. These continuous spatial variations are sufficient to account for the observed spectra, and no additional localization of an injection region is needed.

In summary, the combined analysis of observations from DE 1 and DE 2 conjunctions and our model calculations has provided a number of results regarding the steady state nature of magnetopause reconnection, the source location of precipitating cusp particles, and our ability to simultaneously model multiple locations in the open magnetosphere using a single set of modeling parameters. Even though the modeled spectra are found to be in general agreement with the observations, there are also a number of differences that indicate areas where improvement is needed. Among these areas are the implementation of more realistic magnetic and electric field models and the imposition of charge neutrality on the open field lines.

Acknowledgments. We would like to acknowledge J. L. Burch as the principal investigator of HAPI and J. D. Winningham as the principal investigator of LAPI. The authors would like to thank E. M. Basinska, S. A. Fuselier, M. Lockwood, W. K. Peterson, P. H. Reiff, and M. F. Smith for numerous discussions. This work was supported by NSF grant ATM-9300832.

The Editor thanks D. C. Delcourt and M. E. Greenspan for their assistance in evaluating this paper.

References

Burch, J. L., Precipitation of low energy electrons at high latitudes: Effects of interplanetary magnetic field and dipole tilt angle, *J. Geophys. Res., 77*, 6696, 1972.

Burch, J. L., Quasi-neutrality in the polar cusp, *Geophys. Res. Lett., 12*, 469, 1985.

Burch, J. L., J. D. Winningham, V. A. Blevins, N. Eaker, W. C. Gibson, and R. A. Hoffman, High-altitude plasma instrument for Dynamics Explorer-A, *Space Sci. Instrum., 5*, 455, 1981.

Cowley, S. W. H., Plasma population in a simple open model magnetosphere, *Space Sci. Rev., 26*, 217, 1980.

Cowley, S. W. H., The causes of convection in the Earth's magnetosphere: A review of developments during the IMS, *Rev. Geophys., 20*, 531, 1982.

Cowley, S. W. H., and C. J. Owen, A simple illustrative model of open flux tube motion over the dayside magnetopause, *Planet. Space Sci., 37*, 1461, 1989.

Cowley, S. W. H., J. P. Morelli, and M. Lockwood, Dependence of convective flows and particle precipitation in the high-latitude dayside ionosphere on the X and Y components of the interplanetary magnetic field, *J. Geophys. Res., 96*, 5557, 1991.

Delcourt, D. C., T. E. Moore, J. A. Sauvaud, and C. R. Chappell, Nonadiabatic transport features in the outer cusp region, *J. Geophys. Res., 97*, 16833, 1992.

Eastman, T. E., and E. W. Hones Jr., Characteristics of the magnetospheric boundary layer as observed by IMP 6, *J. Geophys. Res. 84*, 2018, 1979.

Gosling, J. T., M. F. Thomsen, S. J. Bame, and C. T. Russell, Accelerated plasma flows at the near-tail magnetopause, *J. Geophys. Res., 91*, 3029, 1986.

Hill, T. W., Rates of mass, momentum, and energy transfer at the magnetopause, in Proceedings of the Magnetospheric Boundary Layers Conference, *Eur. Space Agency Spec. Publ., 148*, 325, 1979.

Hill, T. W., and P. H. Reiff, Evidence of magnetospheric cusp proton acceleration by magnetic merging at the dayside magnetopause, *J. Geophys. Res., 82*, 3623, 1977.

Hoffman, R. A., and E. R. Schmerling, Dynamics explorer program: an overview, *Space Sci. Instrum., 5*, 345, 1981.

Liu, C., J. D. Perez, T. E. Moore, and C. R. Chappell, Low energy particle signature of substorm dipolarization, *Geophys. Res. Lett., 21*, 229, 1994.

Lockwood, M., and M. F. Smith, The variation of reconnection rate at the dayside magnetopause and cusp ion precipitation, *J. Geophys. Res., 97*, 14841, 1992.

Lockwood, M., and M. F. Smith, Comment on "Mapping the dayside ionosphere to the magnetosphere according to particle precipitation characteristics" by Newell and Meng, *Geophys. Res. Lett., 20*, 1739, 1993.

Lockwood, M., and M. F. Smith, Low- and mid-altitude cusp particle signatures for general reconnection rate variations, 1, Theory, *J. Geophys. Res., 99*, 8531, 1994.

Mauk, B. H. and C.-I. Meng, The aurora and middle magnetospheric processes, in *Auroral Physics*, edited by C.-I. Meng, M. J. Rycroft and L. A. Frank, p. 223, Cambridge University Press, New York, 1991.

Maynard, N. C., T. L. Aggson, E. M. Basinska, W. J. Burke, P. Craven, W. K. Peterson, M. Sugiura, and D. R. Weimer, Magnetospheric boundary dynamics: DE 1 and DE 2 observations near the magnetopause and cusp, *J. Geophys. Res., 96*, 3505, 1991.

Menietti, J. D., and J. L. Burch, Spatial extent of the plasma injection region in the cusp-magnetosheath interface, *J. Geophys. Res., 93*, 105, 1988.

Menietti, J. D., and M. F. Smith, Inverted Vs spanning the cusp boundary layer, *J. Geophys. Res. 98*, 11391, 1993.

Newell, P. T., and C.-I. Meng, The cusp and the cleft/boundary layer: Low-altitude identification and statistical local time variation, *J. Geophys. Res., 93*, 14549, 1988.

Newell, P. T., and C.-I. Meng, Mapping the dayside ionosphere to the magnetosphere according to particle precipitation characteristics, *Geophys. Res. Lett., 19*, 609, 1992.

Newell, P. T., and C.-I. Meng, Reply to comment by Lockwood and Smith, *Geophys. Res. Lett., 20*, 1741, 1993.

Newell, P. T., W. J. Burke, C.-I. Meng, E. R. Sanchez, and M. E. Greenspan, Identification and observations of the plasma mantle at low altitude, *J. Geophys. Res., 96*, 35, 1991a.

Newell, P. T., W. J. Burke, E. R. Sanchez, C.-I. Meng, M. E. Greenspan, and C. R. Clauer, The low-latitude boundary layer and the boundary plasma sheet at low altitude: Prenoon precipitation regions and convection reversal boundaries, *J. Geophys. Res., 96*, 21013, 1991b.

Nishida, A., T. Mukai, H. Hayakawa, N. Kaya, and M. Fujimoto, Precipitation of solar wind like ions in the polar cap during northward interplanetary magnetic field, *J. Geophys. Res., 98*, 11449, 1993.

Onsager, T. G., C. A. Kletzing, J. B. Austin, and H. MacKiernan, Model of magnetosheath plasma in the magnetosphere: Cusp and mantle particles at low-altitudes, *Geophys. Res. Lett., 20*, 479, 1993.

Phillips, J. L., S. J. Bame, R. C. Elphic, J. T. Gosling, M. F. Thomsen, and T. G. Onsager, Well-resolved observations by ISEE 2 of ion dispersion in the magnetospheric cusp, *J. Geophys. Res., 98*, 13429, 1993.

Reiff, P. H., T. W. Hill, and J. L. Burch, Solar wind injection at the dayside magnetospheric cusp, *J. Geophys. Res., 82*, 479, 1977.

Rosenbauer, H., H. Grünwaldt, M. D. Montgomery, G. Paschmann, and N. Sckopke, HEOS 2 plasma observations in the distant polar magnetosphere: The plasma mantle, *J. Geophys. Res., 80*, 2723, 1975.

Sergeev, V. A., and T. Bösinger, Particle dispersion at the nightside boundary of the polar cap, *J. Geophys. Res., 98*, 233, 1993.

Shelly, E. G., R. D. Sharp, and R. G. Johnson, He^{++} and H^{+} flux measurements in the dayside cusp: Estimates of convection electric field, *J. Geophys. Res., 81*, 2363, 1976.

Sonnerup, B. U. Ö., G. Paschmann, I. Papamastorakis, N. Sckopke, G. Haerendel, S. J. Bame, J. R. Asbridge, J. T. Gosling, and C. T. Russell, Evidence for magnetic field reconnection at the Earth's magnetopause, *J. Geophys. Res., 86*, 10049, 1981.

Speiser, T. W., Particle trajectories in model current sheets I. Analytical solutions., *J. Geophys. Res., 70*, 4219, 1965.

Spreiter, J. R., and S. S. Stahara, Magnetohydrodynamic and gasdynamic theories for planetary bow waves, in *Collisionless Shocks in the Heliosphere: Reviews of Current Research, Geophys. Monogr. Ser.*, vol. 35, edited by B. T. Tsurutani and R. G. Stone, p. 85, AGU, Washington, D. C., 1985.

Stern, D. P., Parabolic harmonics in magnetospheris modeling: The main dipole and the ring current, *J. Geophys. Res., 90*, 10851, 1985.

Winningham, J. D., and W. L. Heikkila, Polar cap auroral electron fluxes observed with Isis 1, *J. Geophys. Res., 79*, 949, 1974.

Winningham, J. D., J. L. Burch, N. Eaker, V. A. Blevins, and R. A. Hoffman, The low altitude plasma instrument, *Space Sci. Instrum., 5*, 465, 1981.

Yamauchi, M., and R. Lundin, A narrow region of electron beams at the poleward edge of the cusp, *J. Geophys. Res., 98*, 7585, 1993.

J. B. Austin, L. X. Janoo, and T. G. Onsager, Institute for the Study of Earth, Oceans, and Space, and the Department of Physics, University of New Hampshire, Durham, NH 03824-3525. (e-mail: onsager@gus.unh.edu)

S.-W. Chang and J. D. Perez, Physics Department, Auburn University, Auburn, AL 36849-5311. (e-mail: perez@physics.auburn.edu)

(Received May 3, 1994; revised October 11, 1994;
accepted October 12, 1994.)